Elucidating Heavy Atom Tunneling Kinetics

Federica Angiolari,[†] Giacomo Mandelli,[‡] Simon Huppert,[¶] Chiara Aieta,[‡] and Riccardo Spezia[*,†]

[†]*Sorbonne Université, Laboratoire de Chimie Théorique, UMR 7616 CNRS, 4 Place Jussieu, 75005 Paris (France)*

[‡]*Dipartimento di Chimica, Universitá degli Studi di Milano, 20133 Milano (Italy)*

[¶]*Sorbonne Université, Institut de Nanosciences de Paris, UMR 7588 CNRS, 4 Place Jussieu, 75005 Paris (France)*

E-mail: riccardo.spezia@sorbonne-universite.fr

Abstract

In this work, we characterize the temperature dependence of kinetic properties in heavy atom tunneling reactions by means of molecular dynamics simulations, including nuclear quantum effects (NQEs) via Path Integral theory. To this end, we consider the prototypical Cope rearrangement of semibullvalene.

The reaction was studied in the 25–300 K temperature range observing that the inclusion of NQEs modifies the temperature behavior of both free energy barriers and dynamical recrossing factors with respect to classical dynamics. Notably, while in classical simulations the activation free energy shows a very weak temperature dependence, it becomes strongly dependent on temperature when NQEs are included. This temperature behavior shows a transition from a regime where the quantum effects are limited and can mainly be traced back to zero point energy, to a low temperature regime where tunneling plays a dominant role. In this regime, the free energy curve literally tunnels below the potential energy barrier along the reaction coordinate, allowing much faster reaction rates.

https://doi.org/10.26434/chemrxiv-2024-wb68d **ORCID:** https://orcid.org/0000-0001-5160-489X Content not peer-reviewed by ChemRxiv. **License:** CC BY-NC-ND 4.0

Finally, the temperature dependence of the rate constants obtained from molecular dynamics simulations was compared with available experimental data and with semi-classical transition state theory calculations, showing comparable behaviors and similar transition temperatures from thermal to (deep) tunneling regime.

Introduction

Tunneling through the reaction barrier can be significant in chemical reactions involving light atoms like hydrogen, but it can also occur when heavier atoms are involved. This phenomenon, called heavy atom tunneling (HAT) was first suggested theoretically[1,2] and later confirmed by experiments.[3–5] Thanks to experimental developments enabling the study of organic reactions at very low temperatures (few Kelvin),[6,7] there is a growing interest in the role of HAT in organic synthesis, as recently reviewed by Castro and Karney.[3]

A prototypical HAT reaction is the Cope rearrangement of semibullvalene,[2,4,8] reported in Scheme 1. Actually, HAT in this reaction was first predicted by Borden and co-workers[2] via small curvature tunneling transition state theory (SCT+TST) calculations[9] and later observed experimentally by Sanders and co-workers who also investigated the impact of substituents on the tunneling.[4,8] The same reaction was previously studied at higher temperatures, obtaining, via Arrhenius and Eyring fits, activation barriers of about 6 kcal/mol.[10,11] The availability of theoretical and experimental data for this reaction in different temperature ranges, together with its relative simplicity, makes it a good candidate for a deeper study on the temperature behavior of kinetic and dynamical reaction properties.

Tunneling is often discussed as a phenomenon which can occur when the internal energy of the system is lower than the barrier between two minima. However, chemical reactions are generally performed at constant temperature, and thus one has to consider all the ro-vibrational states thermally available. The path integral (PI) formulation of quantum statistical mechanics[12,13] is naturally expressed in the canonical ensemble and can thus provide a direct picture of how the free energy profile along the reaction coordinate is affected by

https://doi.org/10.26434/chemrxiv-2024-wb68d ORCID: https://orcid.org/0000-0001-5160-489X Content not peer-reviewed by ChemRxiv. License: CC BY-NC-ND 4.0

quantum effects, in particular when tunneling is relevant.

In general, two nuclear quantum phenomena can modify chemical reactivity and reaction rates: vibrational quantization and tunneling. The interplay between temperature and vibrational quantization can be at the origin of a temperature-dependent activation barrier as illustrated in our recent work applying path integral molecular dynamics[14,15] (PI-MD) simulations to the study of unimolecular fragmentation.[16] Methods derived from PI theory such as centroid molecular dynamics[17] and ring-polymer molecular dynamics[18] (RPMD) have early been applied to proton transfer reactions[19] then extensively used to successfully treat tunneling in chemical reactions involving light atoms.[20–26] Though exact simulation of the quantum dynamics of a reaction remains out of reach even for relatively simple molecular systems, theoretical arguments based on semi-classical theory[27] clarify how PI methods can provide remarkably good estimations of reaction rates even lower than the so-called crossover temperature below which tunneling is expected to play a dominant role.[28,29]

In this work we employ the RPMD approach to study the temperature behavior of free energy barriers and the deviations from the transition state theory (TST) by evaluating the so-called recrossing factors. We extend the use of this method to HAT thanks to the possibility of treating the Cope rearrangement of semibulllvalene with tight binding density functional theory (DFTB).[30] As detailed in the Supporting Information (SI), the 3OB parametrization[31] of DFTB provides a picture of the reaction potential energy surface that is similar to what is obtained by higher level calculations which cannot be used in molecular dynamics. The use of RPMD to evaluate kinetics is an appealing topic that rises a growing interest thanks to its broad generality and the possibility to apply it to complex chemical reactions using the typical Cartesian representation of molecular systems and thus on-the-fly approaches to obtain energies and gradients.

https://doi.org/10.26434/chemrxiv-2024-wb68d **ORCID:** https://orcid.org/0000-0001-5160-489X Content not peer-reviewed by ChemRxiv. **License:** CC BY-NC-ND 4.0

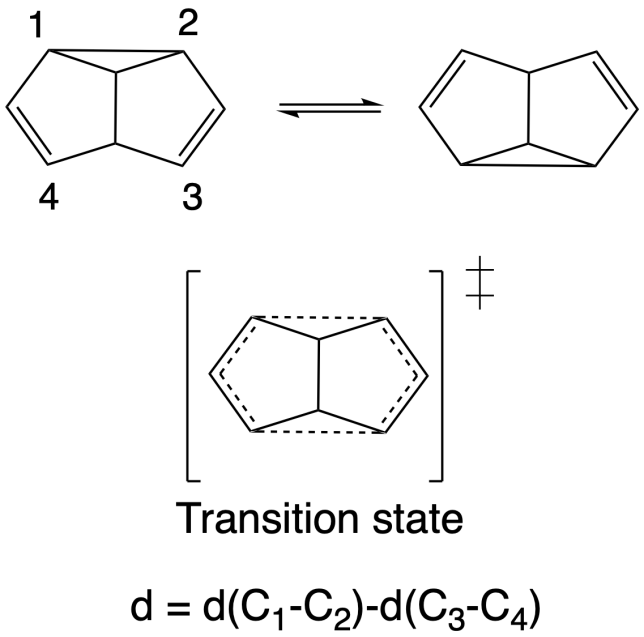

Scheme 1: Cope rearrangement of semibullvalene with atom numbering used in this study. The transition state structure is also depicted. d denotes the reaction coordinate used to describe the reaction, where $d(C_1 - C_2)$ and $d(C_3 - C_4)$ are the distances between atoms C_1 and C_2 and C_3 and C_4, respectively.

Results and Discussion

Free energy profile

By coupling classical (CLMD) and RPMD simulations with the Umbrella Sampling (US) technique[32] it is possible to obtain the free energy profile as a function of the reaction coordinate, which, in the present case, is the difference between C_1-C_2 and C_3-C_4 distances (see 1). Free energy profiles as a function of the reaction coordinate, d, are obtained at different temperatures using both CLMD and RPMD US simulations and reported in Figure 1. As expected, they present a symmetric double well shape, with some interesting differences when NQEs are considered. Notably, while the classical free energies change only very weakly as a function of temperature, they show a significant temperature dependence when including NQEs. The barrier height decreases, and its shape becomes flatter and flatter as the temperature lowers. In particular, at very low temperatures (50 and 25 K), the

https://doi.org/10.26434/chemrxiv-2024-wb68d ORCID: https://orcid.org/0000-0001-5160-489X Content not peer-reviewed by ChemRxiv. License: CC BY-NC-ND 4.0

curves show an essentially flat plateau in an extended TS region.

This characteristic behavior is often observed in PI-based simulations in the tunneling regime.[19,33] In this formalism, each of the atoms composing the system is replicated a large number of times, with the neighboring replicas tied together by harmonic forces. The replicas (also called beads) thus form a cyclic structure, designated as ring polymer. At low temperatures, the harmonic forces become so loose, that the polymer can spread over both reactant and product sides. In other terms, the quantum delocalization becomes more and more important with decreasing temperature as the beads spread over larger and larger regions.

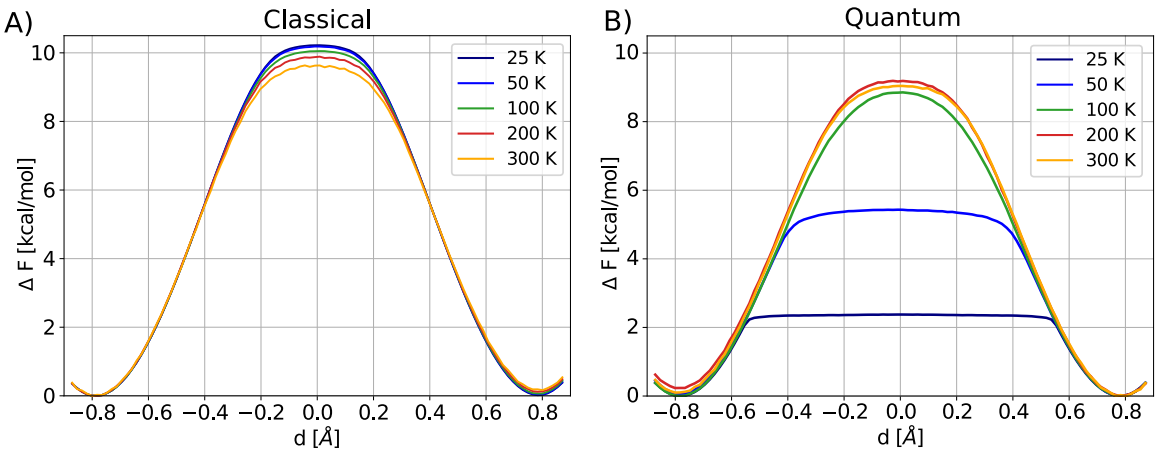

Figure 1: Free energy curves as a function of reaction coordinate, d, at different temperatures, as obtained from classical (panel A) and quantum (RPMD, panel B) Umbrella Sampling simulations.

From such free energy curves, we extracted the free energy barriers (as the difference between reactant and TS points) and reported them in Table 1. Notably, the inclusion of NQEs decreases the free energy barriers, as already visible in 1. Comparing classical and RPMD barriers, we notice that, while the difference is almost negligible at 300 K, it reaches almost 8 kcal/mol at 25 K.

This temperature behavior can be compared with that expected by evaluating the average energy difference as a function of temperature in the harmonic approximation. In fact,

https://doi.org/10.26434/chemrxiv-2024-wb68d ORCID: https://orcid.org/0000-0001-5160-489X Content not peer-reviewed by ChemRxiv. License: CC BY-NC-ND 4.0

Table 1: Free energy barriers as obtained from classical, $\Delta F^{\ddagger}_{Cl}$ and quantum, $\Delta F^{\ddagger}_{Q}$, (using RPMD) Umbrella Sampling simulations at different temperatures (values are in kcal/mol). Classical (κ_{Cl}) and RPMD (κ_{Q}) recrossing factors are also reported.

Temperature [K]	$\Delta F^{\ddagger}_{Cl}$ [kcal/mol][a]	$\Delta F^{\ddagger}_{Q}$ [kcal/mol][a]	κ_{Cl}[b]	κ_{Q}[b]
25	10.2	2.4	0.99	0.63
50	10.2	5.5	0.98	0.94
100	10.1	8.8	0.96	0.97
200	9.9	9.2	0.93	0.96
300	9.7	9.1	0.92	0.93

[a] Statistical uncertainty is estimated at about 0.1 kcal/mol [b] Recrossing factors obtained for the t $\rightarrow \infty$ limit.

knowing the harmonic frequencies of reactant and TS, it is possible to obtain both classical and quantum average vibrational energies and thus average energy barriers: they can provide a simple probe of zero-point energy effect.[16]

In 2, we plot the energy barriers as a function of temperature, as obtained from US simulations and from the harmonic approximation. We can notice that US simulation results follow the harmonic approximation values at high temperatures (300, 200 and 100 K), both in the classical and in the quantum case. On the contrary, at lower temperatures, the RPMD-US barriers diverge from the harmonic approximation ones. Note that for T $\rightarrow$ 0 the difference between classical and quantum results in the harmonic approximation correspond to the reactant-TS ZPE difference, which for the present system is 1.38 kcal/mol. Simulations at 50 and 25 K show a quantum-classical difference which is much higher than the ZPE difference. This is a first evidence that, for temperatures lower than 100 K, HAT starts to play an important role.

In semi-classical theory, it is possible to identify the so-called crossover temperature below which tunneling is expected to provide a dominant contribution to the reaction rate:[29,34,35]

$$T_c = \frac{\hbar \omega^{\ddagger}}{2\pi k_B} \tag{1}$$

where $\omega^{\ddagger}$ is the imaginary frequency (in absolute value) at the transition state, k_B is the Boltzmann constant and $\hbar$ is the reduced Plank constant. For semibullvalene, using 3OB

https://doi.org/10.26434/chemrxiv-2024-wb68d ORCID: https://orcid.org/0000-0001-5160-489X Content not peer-reviewed by ChemRxiv. License: CC BY-NC-ND 4.0

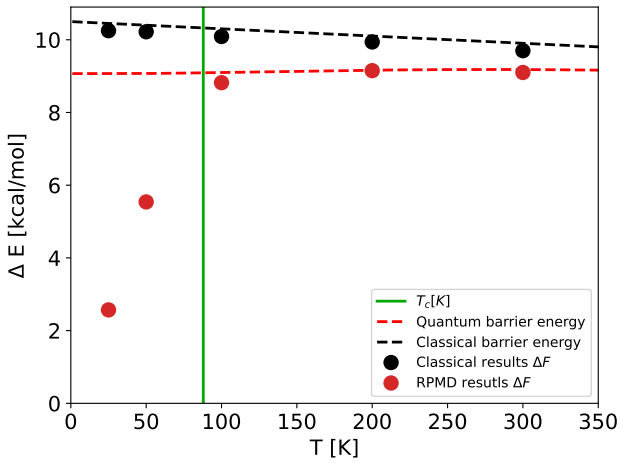

Figure 2: Energy barrier as a function of temperature as obtained by simulations (both CLMD and RPMD US) and from average energy difference between reactant and TS in the harmonic approximation. As vertical line we also report the crossover temperature. All calculations were performed using DFTB with the 3OB parametrization.

DFTB parametrization, we obtain $\omega^{\ddagger} = 413$ cm^{-1}, corresponding to $T_c = 94$ K.

Nicely, while for $T > T_c$ the nuclear quantum effects on the barrier can be mainly attributed to ZPE, simulation data diverge for $T < T_c$, i.e. for 50 and 25 K, which confirms the importance of tunneling. In terms of quantum free energy profiles this corresponds to the appearance of a plateau in the TS region instead of a sharp curve as for higher temperatures. Notably, this plateau acts as a tunnel: the reaction follows a free energy path that passes through the potential energy hill. Even if this plateau retains some curvature, it could tend to a perfectly flat curve for T $\rightarrow$ 0. Unfortunately, the number of beads required to converge RPMD simulations increases with decreasing T, which makes simulations at temperatures lower than 25K practically unfeasible.

Recrossing factors

The free energy profile as a function of the reaction coordinate provides the key ingredient to obtain the rate constant in the TST theory. In such a theory, one key assumption is the fact that once the system reaches the TS with a non-zero momentum towards the product

https://doi.org/10.26434/chemrxiv-2024-wb68d **ORCID:** https://orcid.org/0000-0001-5160-489X Content not peer-reviewed by ChemRxiv. **License:** CC BY-NC-ND 4.0

state, its fate is to go to the product state. However, it is possible that some trajectories recross back to the reactant. As a consequence, the microscopic rate constant can be written as:[21,36]

$$k(T) = \kappa(T) k^{TST}(T) \tag{2}$$

where $k^{TST}(T)$ is the TST rate constant and $\kappa(T)$ the recrossing factor (which is temperature dependent). Note that RPMD rate theory reads exactly the same, only the recrossing factor is obtained from the ring-polymer centroid dynamics.[21,37] From simulations the recrossing factor can be obtained (see SI for details) and from its microscopic definition it is not only temperature but also time dependent.[22,33,37] The long-time value is then used to correct the TST rate constant.

CLMD and RPMD recrossing factors as a function of time at different temperatures are reported in Figure 3. For T = 100 K and above, the classical and RPMD behaviors are very similar while the picture clearly changes at 50 K and, even more strikingly, at 25 K. In classical simulations, decreasing the temperature causes a slight increase of κ towards 1. Indeed, classically, there is less energy exchange from the reaction coordinate to other vibration modes at low temperature than at high temperature, and this energy redistribution is at the origin of recrossing. The same is observed in RPMD simulations above the crossover temperature.

However, at lower temperatures, κ values obtained from RPMD simulations decrease when temperature decreases, in correspondence with the abrupt change in the free energy profiles and the emergence of HAT driven reactivity. This is summarized in 1 where we report the different κ values obtained from both CLMD and RPMD simulations at "infinite" time (i.e. the converged values shown in 3). As discussed previously, the free energy profile is almost flat at lower temperatures and thus the trajectories can more easily cross the TS back and forth. The strongest effect is obtained at 25 K, at which the free energy profile is the flattest: firstly, the equilibration in time of κ is much slower than previously (almost 2 ps

https://doi.org/10.26434/chemrxiv-2024-wb68d ORCID: https://orcid.org/0000-0001-5160-489X Content not peer-reviewed by ChemRxiv. License: CC BY-NC-ND 4.0

are needed, as shown in Figure 3), and secondly, the final value is about 0.6 which means that about 40% of the trajectories undergo multiple crossings of the TS.

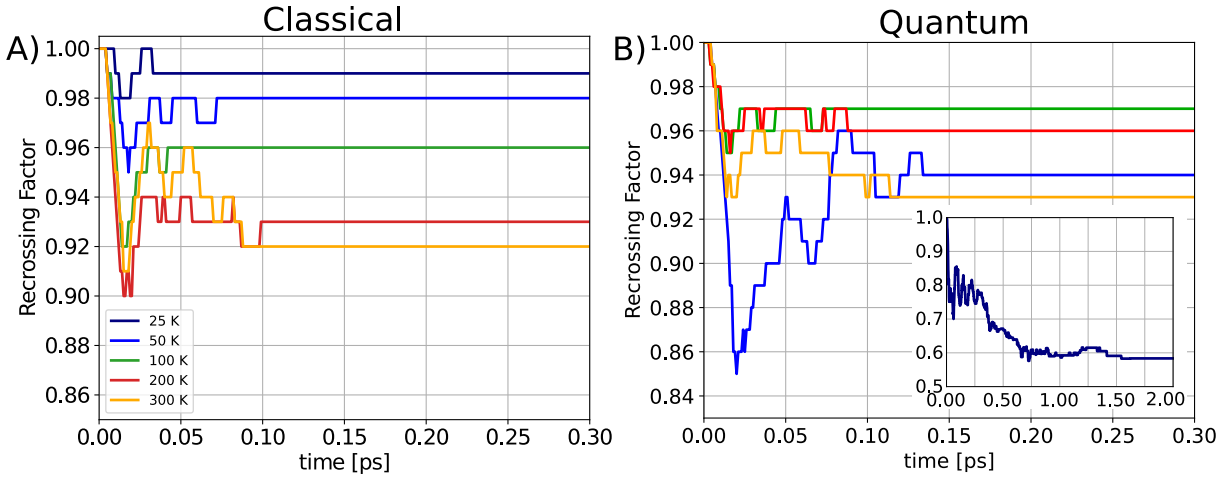

Figure 3: Recrossing factors as function of time at different temperatures: A) Classical simulations, B) RPMD simulations. In the inset of panel B we show the RPMD results at 25 K.

Rate Constants

Once determined the free energy profiles and the recrossing factors from molecular simulations (both classical and quantum) it is possible to compute the full rate constants at different temperatures simply from 2. The TST rate constants, both classical and quantum (using the RPMD formalism), can be obtained from the free energy profile as a function of the reaction coordinate.[21,22,33] Details on how the different $k^{TST}(T)$ are obtained from simulations are given in the Supporting Information.

Classical and quantum (RPMD) results are shown in an Arrhenius plot in 4. First, we can compare the classical and the quantum temperature-behavior: at 300 and 200 K the two rate constants are very similar, while they begin to diverge at 100 K and more strongly at 50 K and 25 K, where the difference becomes huge. In fact, while classical rates show an almost linear behavior in 4 (as expected by the simple Arrhenius rate equation in which the temperature dependence of the activation energy is disregarded[38]), the quantum rates reach

https://doi.org/10.26434/chemrxiv-2024-wb68d ORCID: https://orcid.org/0000-0001-5160-489X Content not peer-reviewed by ChemRxiv. License: CC BY-NC-ND 4.0

a plateau at low temperatures which is a typical sign of tunneling, and corresponds to what is observed experimentally.[4,10] Quantitatively, the inclusion of NQEs increases the rates at low temperature up to 70 orders of magnitude (see values reported in the SI).

We also computed the rate constants via the quantum harmonic TST (see details in SI), that only accounts for ZPE effects but cannot capture tunneling by construction. The resulting values are only slightly higher than the classical ones, while RPMD rates are orders of magnitude faster. This data shows that molecular simulations, including NQEs via path integral theory, can describe tunneling beyond H transfer, also for reactions involving heavy atoms. As for the free energy barrier and recrossing factor, the plateau is reached around the crossover temperature.

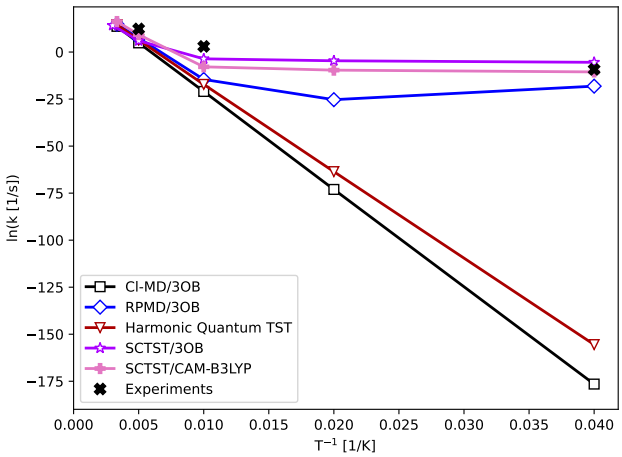

Figure 4: Rate constants for the Cope rearrangement of semibullvalene as obtained from Classical (Cl-MD) and RPMD simulations with 3OB DFTB parameters and SCTST theory using either 3OB DFTB or DFT with the CAM-B3LYP functional. Experimental data are taken from Ref.[10] (at 200 and 100 K) and Ref.[4] (for methyl-semibullvalene at 25 K). All the numerical values are reported in the SI.

The reaction rate seems to show a slight (and unphysical) increase from 50 to 25K, but this difference is within the uncertainty of our simulations. Indeed, a very small increase of 0.4 kcal/mol of the free energy barrier at 25K is sufficient to reduce the rate to a value of the same order as that obtained at 50K (see SI for details).

Rate constants were also calculated using the semi-classical TST (SCTST) as recently de-

https://doi.org/10.26434/chemrxiv-2024-wb68d **ORCID:** https://orcid.org/0000-0001-5160-489X Content not peer-reviewed by ChemRxiv. **License:** CC BY-NC-ND 4.0

veloped by Aieta, Ceotto and co-workers (details are given in the SI).[39–41] This approach was recently used to study HAT of simpler chemical reactions,[41] and it was successfully applied with high accuracy in the study of cryogenic reactions.[42] The SCTST approach requires the calculation of energy, harmonic frequencies, and anharmonic normal mode couplings for the reactant and the TS. In principle, this is doable for any molecule; however, new implementations have been devised to overcome practical issues when applying the method to large molecules.[43] Here, we could calculate the anharmonic vibrational density of states to obtain the rate constant using 3OB DFTB parametrization[31] and the CAM-B3LYP functional[44] with the 6-311++G(d,p) basis set. This last method was chosen as it yields barriers similar to that of highly correlated calculations (see SI). The corresponding rate constants are reported in the same 4 for comparison. As expected, the 3OB SCTST rates are very similar to both classical and RPMD rates from molecular dynamics at high temperatures. Decreasing the temperature they converge to slightly higher values with a plateau reached already at 100 K. Using the CAM-B3LYP functional yields slightly lower rate constants than with the 3OB method.

Experimental values are reported for the semibullvalene at 200 and 100 K,[10] while only the methyl-semibullvalene was studied experimentally at 25 K[4](experiments were done also at lower temperatures but in this very deep tunneling regime both RPMD simulations and SCTST are not guaranteed to provide trustworthy results[42]). Experimental data are very close to the CAM-B3LYP SCTST results over the whole temperature range, reflecting that this functional is able to very well describe the TS energy and vibrational properties. Notably, when comparing with the results obtained with DFTB (3OB parametrization), the experimental point at 25 K is situated in between the SCTST and the RPMD values: it is well known that, for symmetric barriers, RPMD underestimates the rate in the (deep) tunneling regime, as observed by Manolopoulos and co-workers[23,24] and theoretically explained by Richardson and Althorpe.[27] On the other hand, the SCTST method overestimates the influence of tunneling in that same regime when applied to one dimensional model po-

https://doi.org/10.26434/chemrxiv-2024-wb68d **ORCID:** https://orcid.org/0000-0001-5160-489X Content not peer-reviewed by ChemRxiv. **License:** CC BY-NC-ND 4.0

tentials.[45] The present RPMD vs SCTST comparison using the same electronic structure method therefore confirms these trends.

Conclusion

Summarizing, in this article we focus on how NQEs affect the temperature dependence of the free energy profile and, consequently, of the rate constant for the prototypical Cope rearrangement of semibulvalene.

From such temperature dependences it is clear that, below the crossover temperature $T_c \sim 100$ K, the main effect on the free energy profile is due to tunneling. We can thus identify two regimes. For $T > T_c$ the main NQE is the vibrational quantization, but the rate is only sightly affected and the behavior in an Arrhenius plot remains linear with a slightly different slope. For $T < T_c$ the situation is totally different; now tunneling starts to be important, the quantum free energy profile is flat and the rate becomes almost temperature independent. This effect is evident in particular at 50 and 25 K, where the Path Integral free energy profile is completely flat in the TS region. This leads to a huge increase of the rate constant, by 70 orders of magnitude compared to the classical one. Notably, the free energy profile in the (deep) tunneling regime resembles a free energy tunnel passing below the hill of the potential energy barrier.

The rate constant temperature dependence is confirmed by semi-classical TST calculations and is in qualitative agreement with experiments. Of course, the theoretical description of the energy barrier is crucial to quantitatively recover the rate values: CAM-B3LYP provides results very close to the experiments, but unfortunately, it cannot be used presently in RPMD simulations due to computational limitations. However, it could be considered in future studies to parametrize computationally cheaper methods, not only in the DFTB context but also, for example, through machine learning potentials.

In conclusion, in the present article we show how powerful Ring Polymer Molecular Dy-

https://doi.org/10.26434/chemrxiv-2024-wb68d **ORCID:** https://orcid.org/0000-0001-5160-489X Content not peer-reviewed by ChemRxiv. **License:** CC BY-NC-ND 4.0

namics simulations can be used to incorporate tunneling effects in reactions which involve heavy atoms. This opens new possibilities and new reactions could be scrutinized theoretically in the future. More in general, two complementary theoretical tools can be employed: (i) semi-classical TST, which requires the evaluation of the anharmonic density of states, (ii) path-integral based MD, that can be employed when molecular dynamics simulations can be afforded and converged. Both are able to correctly account for heavy atom tunneling.

Acknowledgements

We thank Prof. Michele Ceotto for useful discussions.

Conflict of Interest

No conflict of interest to declare.

References

(1) Carpenter, B. K. *J. Am. Chem. Soc.* **1983**, *105*, 1700–1701.

(2) Zhang, X.; Hrovat, D. A.; Borden, W. T. *Org. Lett.* **2010**, *12*, 2798–2801.

(3) Castro, C.; Karney, W. L. *Angew. Chem. Int. Ed.* **2020**, *59*, 8355–8366.

(4) Schleif, T.; Tatchen, J.; Rowen, J. F.; Beyer, F.; Sanchez-Garcia, E.; Sander, W. *Chem. Eur. J.* **2020**, *26*, 10452–10458.

(5) Gonzalez-James, O. M.; Zhang, X.; Datta, A.; Hrovat, D. A.; Borden, W. T.; Singleton, D. A. *J. Am. Chem. Soc.* **2010**, *132*, 12548–12549.

(6) Ertelt, M.; Hrovat, D. A.; Borden, W. T.; Sander, W. *Chem. Eur. J.* **2014**, *20*, 4713–4720.

(7) Henkel, S.; Ertelt, M.; Sander, W. *Chem. Eur. J.* **2014**, *20*, 7585–7588.

https://doi.org/10.26434/chemrxiv-2024-wb68d **ORCID:** https://orcid.org/0000-0001-5160-489X Content not peer-reviewed by ChemRxiv. **License:** CC BY-NC-ND 4.0

(8) Schleif, T.; Mieres-Perez, J.; Henkel, S.; Ertelt, M.; Borden, W. T.; Sander, W. *Angew. Chem. Int. Ed.* **2017**, *56*, 10746–10749.

(9) Skodje, R. T.; Truhlar, D. G.; Garrett, B. C. *J. Phys. Chem.* **1981**, *85*, 3019–3023.

(10) Cheng, A. K.; Anet, F. A. L.; Mioduski, J.; Meinwald, J. *J. Am. Chem. Soc.* **1974**, *96*, 2887–2891.

(11) Moskau, D.; Aydin, R.; Leber, W.; Giinther, H.; Quast, H.; Martin, H.-D.; Hassenrick, K.; Miller, L. S.; Grohmann, K. *Chem. Ber.* **1989**, *122*, 925–931.

(12) Feynman, R. P.; Hibbs, A. R. *Quantum Mechanics and Path Integrals*; McGraw Hill: New York, 1965.

(13) Berne, B. J. *J. Stat. Phys.* **1986**, *43*, 911–929.

(14) Marx, D.; Parrinello, M. *J. Chem. Phys.* **1996**, *104*, 4077–4082.

(15) Tuckerman, M. E. *Statistical mechanics: theory and molecular simulation*; Oxford university press, 2023.

(16) Angiolari, F.; Huppert, S.; Spezia, R. *Phys. Chem. Chem. Phys.* **2022**, *24*, 29357–29370.

(17) Cao, J.; Voth, G. A. *J. Chem. Phys.* **1993**, *99*, 10070–10073.

(18) Craig, I. R.; Manolopoulos, D. E. *J. Chem. Phys.* **2004**, *121*, 3368–3373.

(19) Hinsen, K.; Roux, B. *J. Chem. Phys.* **1997**, *106*, 3567–3577.

(20) Craig, I. R.; Manolopoulos, D. E. *J. Comput. Phys.* **2005**, *122*, 084–106.

(21) Craig, I. R.; Manolopoulos, D. E. *J. Comput. Phys.* **2005**, *123*, 034102.

(22) Collepardo-Guevara, R.; Craig, I.; Manolopoulos, D. *J. Chem. Phys.* **2008**, *128*, 144502.

(23) Collepardo-Guevara, R.; Suleimanov, Y. V.; Manolopoulos, D. E. *J. Comput. Phys.* **2009**, *130*, 174713.

(24) Suleimanov, Y. V.; Collepardo-Guevara, R.; Manolopoulos, D. *J. Chem. Phys.* **2011**, *134*, 044131.

(25) Zhang, L.; Zuo, J.; Suleimanov, Y. V.; Guo, H. *J. Phys. Chem. Lett.* **2023**, *14*, 7118–7125.

(26) Angiolari, F.; Huppert, S.; Pietrucci, F.; Spezia, R. *J. Phys. Chem. Lett.* **2023**, *14*,

https://doi.org/10.26434/chemrxiv-2024-wb68d **ORCID:** https://orcid.org/0000-0001-5160-489X Content not peer-reviewed by ChemRxiv. **License:** CC BY-NC-ND 4.0

5102–5108.

(27) Richardson, J. O.; Althorpe, S. C. *J. Chem. Phys.* **2009**, *131*, 214106.

(28) Benderskii, V. A.; Makarov, D. E.; Wight, C. A. *Adv. Chem. Phys.* **1994**, *88*, 55.

(29) Christov, S. G. *Mol. Eng.* **1997**, *7*, 109–147.

(30) Elstner, M.; Porezag, D.; Jungnickel, G.; Elsner, J.; Haugk, M.; Frauenheim, T.; Suhai, S.; Seifert, G. *Phys. Rev. B* **1998**, *58*, 7260–7268.

(31) Gaus, M.; Goez, A.; Elstner, M. *J. Chem. Theory Comput.* **2013**, *9*, 338–354.

(32) Torrie, G.; Valleau, J. *J. Comput. Phys.* **1977**, *23*, 187–199.

(33) Suleimanov, Y. V. *J. Phys. Chem. C* **2012**, *116*, 11141–11153.

(34) Gillan, M. J. *J. Phys. C: Solid State Phys.* **1987**, *20*, 3621.

(35) Alvarez-Barcia, S.; Flores, J. R.; Kastner, J. *J. Phys. Chem. A* **2014**, *118*, 78–82.

(36) Chandler, D. *J. Chem. Phys.* **1978**, *68*, 2959–2970.

(37) Suleimanov, Y. V.; Aoiz, F. J.; Guo, H. *J. Phys. Chem. A* **2016**, *120*, 8488–8502.

(38) Truhlar, D. G. *J. Chem. Educ.* **1978**, *55*, 309–311.

(39) Aieta, C.; Gabas, F.; Ceotto, M. *J. Phys. Chem. A* **2016**, *120*, 4853–4862.

(40) Aieta, C.; Gabas, F.; Ceotto, M. *J. Chem. Theory Comput.* **2019**, *15*, 2142–2153.

(41) Mandelli, G.; Aieta, C.; Ceotto, M. *J. Chem. Theory Comput.* **2022**, *18*, 623–637.

(42) Mandelli, G.; Corneo, L.; Aieta, C. *J. Phys. Chem. Lett.* **2023**, *14*, 9996–10002.

(43) MultiWell-2023 Software Suite; J. R. Barker, University of Michigan, Ann Arbor, Michigan, USA, 2023. http://clasp-research.engin.umich.edu/multiwell/.

(44) Yanai, T.; Tew, D.; Handy, N. *Chem. Phys. Lett.* **2004**, *393*, 51–57.

(45) Goel, P.; Stanton, J. F. *J. Chem. Phys.* **2018**, *149*, 134109.

https://doi.org/10.26434/chemrxiv-2024-wb68d **ORCID:** https://orcid.org/0000-0001-5160-489X Content not peer-reviewed by ChemRxiv. **License:** CC BY-NC-ND 4.0